BIOCHEMISTRY
including biophysical chemistry & molecular biology

ARTICLE

pubs.acs.org/biochemistry

Probing Domain Interactions in Soluble Guanylate Cyclase

Emily R. Derbyshire,[†,#] Michael B. Winter,[‡] Mohammed Ibrahim,[∥,▽] Sarah Deng,[§] Thomas G. Spiro,[∥] and Michael A. Marletta[*,†,‡,⊥,@]

[†]Department of Molecular and Cell Biology, [‡]Department of Chemistry, and [§]Department of Plant and Microbial Biology, University of California, Berkeley, California 94720, United States

[∥]Department of Chemistry, University of Washington, Seattle, Washington 98195-1700, United States

[⊥]California Institute for Quantitative Biosciences and [@]Division of Physical Biosciences, University of California, Berkeley, California 94720-3220, United States

Supporting Information

ABSTRACT: Eukaryotic nitric oxide (NO) signaling involves modulation of cyclic GMP (cGMP) levels through activation of the soluble isoform of guanylate cyclase (sGC). sGC is a heterodimeric hemoprotein that contains a Heme−Nitric oxide and OXygen binding (H-NOX) domain, a Per/ARNT/Sim (PAS) domain, a coiled-coil (CC) domain, and a catalytic domain. To evaluate the role of these domains in regulating the ligand binding properties of the heme cofactor of NO-sensitive sGC, we constructed chimeras by swapping the rat β1 H-NOX domain with the homologous region of H-NOX domain-containing proteins from *Thermoanaerobacter tengcongensis*, *Vibrio cholerae*, and *Caenorhabditis elegans* (*Tt*Tar4H, VCA0720, and Gcy-33, respectively). Characterization of ligand binding by electronic absorption and resonance Raman spectroscopy indicates that the other rat sGC domains influence the bacterial and worm H-NOX domains. Analysis of cGMP production in these proteins reveals that the chimeras containing bacterial H-NOX domains exhibit guanylate cyclase activity, but this activity is not influenced by gaseous ligand binding to the heme cofactor. The rat−worm chimera containing the atypical sGC Gcy-33 H-NOX domain was weakly activated by NO, CO, and O_2, suggesting that atypical guanylate cyclases and NO-sensitive guanylate cyclases have a common molecular mechanism for enzyme activation. To probe the influence of the other sGC domains on the mammalian sGC heme environment, we generated heme pocket mutants (Pro118Ala and Ile145Tyr) in the β1 H-NOX construct (residues 1−194), the β1 H-NOX-PAS-CC construct (residues 1−385), and the full-length α1β1 sGC heterodimer (β1 residues 1−619). Spectroscopic characterization of these proteins shows that interdomain communication modulates the coordination state of the heme−NO complex and the heme oxidation rate. Taken together, these findings have important implications for the allosteric mechanism of regulation within H-NOX domain-containing proteins.

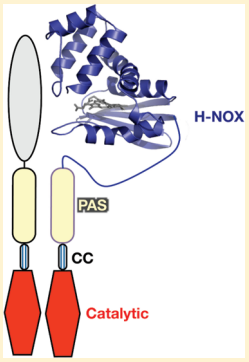

Soluble guanylate cyclases (sGCs) are heterodimeric hemoproteins that respond to gaseous signaling molecules. The best-characterized eukaryotic sGCs contain a heme cofactor that rapidly binds nitric oxide (NO) but does not bind oxygen (O_2). Additionally, the heme iron is stable in the ferrous oxidation state. This selective binding of NO allows the protein to function as an essential NO sensor in mammals. Worms and flies are known to contain atypical sGCs that are distinct from mammalian sGC as they bind and respond to O_2 in addition to NO and carbon monoxide (CO). Despite these differences in ligand selectivity, both non-O_2-binding and O_2-binding sGCs play critical physiological roles by synthesizing cyclic GMP (cGMP).[1−4]

The best-characterized non-O_2-binding sGC heterodimer is the rat α1β1 protein. The α1 and β1 subunits are highly homologous, and both proteins consist of four distinct domains (reviewed in ref 5). The β1 subunit, which is the heme-binding subunit, contains an N-terminal Heme−Nitric Oxide and OXygen binding (H-NOX) domain, a Per/ARNT/Sim (PAS) domain, a coiled-coil (CC) domain, and a C-terminal catalytic domain (Figure 1A). Predicted O_2-binding sGCs from *Drosophila* and *Caenorhabditis elegans* also contain H-NOX, PAS, CC, and catalytic domains on the basis of primary sequence analysis.

Previously characterized heme binding truncations of the β1 subunit include the H-NOX construct β1(1−194)[6] and the H-NOX-PAS-CC construct β1(1−385).[7] Several bacterial H-NOX proteins with homology to β1(1−194) have been characterized. These homologues are not fused to guanylate cyclase domains but are thought to be involved in gaseous signaling. Some H-NOX domain homologues are fused to predicted methyl-accepting chemotaxis proteins, like the O_2-binding H-NOX domain from *Thermoanaerobacter tengcongensis*, while others are associated with histidine kinases, like the H-NOX protein from *Vibrio cholerae*, or diguanylate cyclases. To date, there is no crystal structure of an H-NOX domain from a guanylate cyclase; however, the structures of three bacterial H-NOX proteins with a high degree of homology

Received: March 7, 2011
Revised: April 11, 2011
Published: April 14, 2011

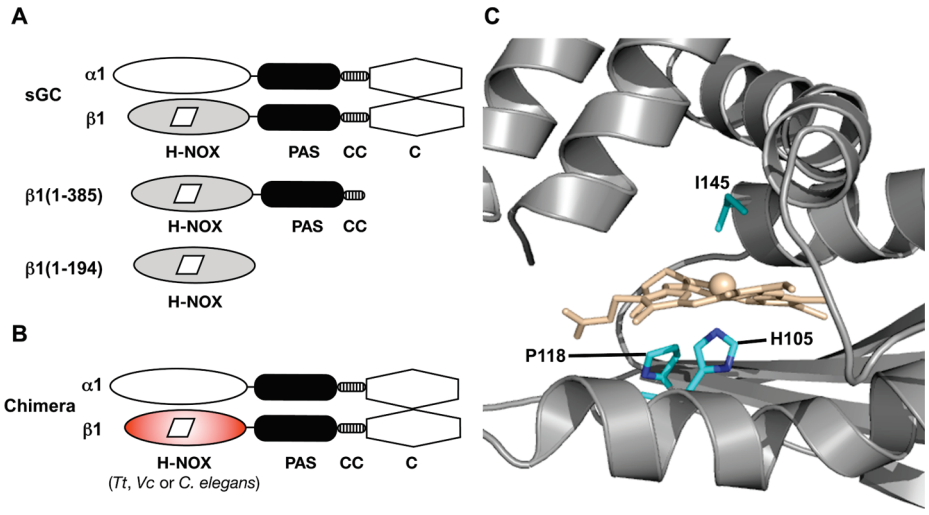

Figure 1. (A) Domain architecture of sGC $\alpha1\beta1$, $\beta1(1-385)$, and $\beta1(1-194)$. H-NOX, PAS, coiled-coil (CC), and catalytic (C) domains are shown. (B) Chimeras contain the *T. tengcongensis*, *V. cholerae*, or *C. elegans* H-NOX domain fused to the rat $\beta1$ PAS, CC, and C domains. (C) Homology model of the rat $\beta1$ H-NOX domain (PDB entry 1U55). Residues in the proximal pocket (His105 and Pro118) and in the distal pocket (Ile145) are shown.

to $\beta1(1-194)$ have been determined.[8−11] These structures have guided many proposals on sGC activation and regulation, yet the precise function of each domain in the mammalian enzyme remains to be determined. Additionally, the functional and structural homology among the bacterial H-NOX proteins, the eukaryotic O_2-binding H-NOX proteins, and the eukaryotic non-O_2-binding H-NOX proteins is unknown. To address these questions, we constructed chimeric proteins by replacing the rat $\beta1$ H-NOX domain with bacterial or eukaryotic H-NOX domains. We found that sensitivity of the enzyme to gaseous ligand binding (NO, O_2, and CO) is observed when the $\beta1$ H-NOX domain is replaced with an atypical guanylate cyclase H-NOX domain from *C. elegans* (Gcy-33), but this sensitivity is abolished by replacement of the sGC heme domain with two of its bacterial homologues (*Tt*Tar4H H-NOX and VCA0720 H-NOX). This suggests that NO-sensitive and atypical guanylate cyclases have a common mechanism of communication between the H-NOX domain and catalytic domains and/or contain domains that exhibit a relatively high degree of structural homology. To further probe the role of the PAS, CC, and catalytic domains in modulating the ligand binding properties of sGC, two residues [Tyr145 and Pro118 (Figure 1C)] known to be important for O_2 binding and/or heme conformation in *Tt* H-NOX[12,13] were mutated in the full-length $\alpha1\beta1$ heterodimer, $\beta1(1-385)$, and $\beta1(1-194)$. Our results with these mutants highlight the allosteric influence that the $\alpha1$ subunit and the $\beta1$ PAS, CC, and catalytic domains have over the heme environment.

MATERIALS AND METHODS

Reagents.. Primers were obtained from Elim Biopharmaceuticals. Sf9 cells were obtained from the Department of Molecular and Cell Biology Tissue Culture Facility (University of California, Berkeley, CA). Diethylammonium (*Z*)-1-(*N*,*N*-diethylamino)diazen-1-ium-1,2-diolate (DEA/NO) was from Cayman Chemical Co.

Generation of sGC Chimeras, Protein Expression, and Purification. Alignments of various H-NOX domains were conducted with MegAlign (LaserGene, DNAStar Inc.) to guide chimera construction. The N-terminal residues of *Tt*Tar4H (1−180), VCA0720 (1−178), and Gcy-33 (1−184) were fused to rat $\beta1$ residues 187−619 for *Tt*_$\beta1$ and Gcy-33_$\beta1$ or residues 181−619 for *Vc*_$\beta1$ and then cloned into pFastBac (Invitrogen). All constructs were verified by sequencing (DNA Sequencing Facility, University of California, Berkeley, CA). For chimera expression, the Bac-to-Bac baculovirus expression system (Invitrogen) was used to generate recombinant baculovirus according to the manufacturer's instructions. Sf9 cells were co-infected with wild-type $\alpha1$ and chimeric $\beta1$ constructs. $\alpha1$/*Tt*_$\beta1$, $\alpha1$/*Vc*_$\beta1$, and $\alpha1$/Gcy-33_$\beta1$ were purified using a previously reported procedure[14] with a few modifications. After elution from the Ni affinity resin, $\alpha1$/*Tt*_$\beta1$ was exchanged into a 0 mM NaCl buffer and then applied to an anion-exchange column. After being washed, the column was developed with a gradient from 0 to 150 mM NaCl in elution buffer. $\alpha1$/*Vc*_$\beta1$ was purified with a substoichiometric amount of heme and reconstituted. To reconstitute the protein, 1.5−2 equiv of hemin was added to the protein and the sample was left on ice for 12 h to allow the reaction mixture to equilibrate. Excess hemin was then removed by applying the protein to a PD-10 column equilibrated with 50 mM Hepes (pH 7.4), 50 mM NaCl, and 5 mM dithiothreitol (DTT). The protein was characterized both as isolated and after heme reconstitution to ensure the procedure did not affect heme ligand binding.

Generation of Mutants, Protein Expression, and Purification. Mutants of rat $\beta1$ (P118A and I145Y) were generated using the QuikChange XL site-directed mutagenesis kit (Stratagene) according to the manufacturer's instructions. The accuracy of each substitution was verified by sequencing (DNA Sequencing Facility).

Rat $\beta1(1-194)$ and $\beta1(1-385)$ were expressed and purified by a method that was slightly modified from an existing protocol.[6] Specifically, constructs were transformed into *Escherichia coli* Tuner(DE3) competent cells. Expression cultures for $\beta1(1-194)$ and $\beta1(1-385)$ were grown at 37 °C to an A_{600} of 0.6−0.7 and then cooled to 20 °C. Protein expression was induced by the addition of IPTG to a final concentration of 0.5 mM, and cultures were supplemented with aminolevulinic acid to a final concentration of 0.1 mM for all constructs except

β1(1−385) P118A, which was induced with 1 mM IPTG in the absence of aminolevulinic acid. Cells were harvested by centrifugation 15−18 h postinduction, and cell pellets were stored at −80 °C. Frozen cell pellets from 2 or 3 L of culture were thawed and resuspended in 50 mL of buffer A [50 mM DEA (pH 8.5), 20 mM NaCl, 5 mM DTT, 1 mM Pefabloc (Pentapharm), and 5% glycerol]. Resuspended cells were lysed with an Emulsiflex-C5 high-pressure homogenizer and centrifuged for 90 min at 100000*g*. The supernatant was applied to a Toyopearl SuperQ 650 M (Tosohaas) anion-exchange column, and a gradient was developed from 20 to 500 mM NaCl. Fractions containing the protein of interest were concentrated and then applied to a prepacked Superdex S75 HiLoad 16/60 gel filtration column (Pharmacia) for β1(1−194) or a prepacked Superdex S200 HiLoad 16/60 gel filtration column (Pharmacia) for β1(1−385). The gel filtration buffer consisted of 50 mM TEA (pH 7.5), 150 mM NaCl, 5 mM DTT, and 5% glycerol. Protein was then pooled, concentrated, and stored at −80 °C. Protein concentrations were determined using the Bradford Microassay (Bio-Rad Laboratories). β1(1−385) P118A, β1(1−385) P118A/I145Y, and β1(1−194) P118A were isolated with a substoichiometric amount of heme and were reconstituted using the method described above for the α1/*Vc*_β1 heme reconstitution. These proteins were characterized both as isolated and after heme reconstitution to ensure the procedure did not affect heme ligand binding.

The Bac-to-Bac baculovirus expression system (Invitrogen) was used to generate recombinant baculovirus according to the manufacturer's protocol for the expression of β1 P118A. Sf9 cells were cultured, and recombinant α1β1 P118A was purified according to a previously published protocol[14] with the following modification. sGC collected from the Ni affinity resin was treated with 1.5 equiv of hemin in 25 mM TEA (pH 7.5), 50 mM NaCl, and 5 mM DTT and placed on ice for 12 h. After this procedure, the protein was applied to an anion-exchange column as reported for the purification of wild-type α1β1.[14] Protein purity was assessed by sodium dodecyl sulfate−polyacrylamide gel electrophoresis (SDS−PAGE) (>95%), and concentrations were determined using the Bradford Microassay (Bio-Rad Laboratories). The protein was characterized both as isolated and after heme reconstitution to ensure the procedure did not affect enzyme activity or ligand binding.

Enzyme Assays. Duplicate end point assays were performed for sGC chimeras at 25 °C and for α1β1 P118A at 37 °C as previously described.[15] Briefly, sGC complexes were formed with DEA/NO (100 μM) or CO gas (Praxair, Inc.) and confirmed with electronic absorption spectroscopy. Assay mixtures for α1β1 P118A contained 0.2 μg of protein, 50 mM Hepes (pH 7.4), 1 mM DTT, 3 mM $MgCl_2$, 1.5 mM GTP, and 150 μM YC-1 (in DMSO) where indicated. Assay mixtures for chimeras contained 0.2−1 μg of protein, 50 mM Hepes (pH 7.4), 50 mM NaCl, 1 mM DTT, 4 mM $MgCl_2$, 2 mM GTP, and 150 μM YC-1 (in DMSO) where indicated. Chimera assays of Fe^{II} or Fe^{II}−CO complexes were conducted in the presence of 100 μM sodium dithionite and limited O_2. All assays were conducted in a final volume of 100 μL and contained 2% DMSO, which was shown not to affect enzyme activity. Reactions were quenched after 2 min for α1β1 P118A or 5 min for sGC chimeras by the addition of 400 μL of 125 mM $Zn(CH_3CO_2)_2$ and 500 μL of 125 mM Na_2CO_3. cGMP quantification was conducted using a cGMP enzyme immunoassay kit, Format B (Biomol), per the manufacturer's instructions. Each experiment was repeated three times to ensure reproducibility.

Table 1. Electronic Absorption Peak Positions for sGC Chimeras at 25 °C

protein	ligand	coordinate	Soret maximum (nm)
α1/β1	as isolated	5	431
	Fe^{II}-unligated	5	431
	Fe^{II}−NO	5	399
	Fe^{II}−CO	6	423
α1/*Tt*_β1	as isolated	6	418−420
	Fe^{II}-unligated	5	432
	Fe^{II}−NO	6	420
	Fe^{II}−CO	6	423
	Fe^{II}−O_2	6	420
α1/*Vc*_β1[a]	as isolated	ND[b]	402/420
	Fe^{II}-unligated	5	426
	Fe^{II}−NO	5	401
	Fe^{II}−CO	6	420
α1/Gcy-33_β1	as isolated	ND[b]	424
	Fe^{II}-unligated	5	433
	Fe^{II}−NO	6	422
	Fe^{II}−CO	6	421
	Fe^{II}−O_2	6	418

[a] α1/*Vc*_β1 reconstituted with heme. [b] Not determined.

Kinetics. The rates of oxidation of β1(1−385) P118A and β1(1−194) P118A were determined using a stopped-flow spectrophotometer (TgK Scientific) at 10 and 37 °C, respectively. Samples of anaerobic Fe^{II}-bound protein were combined with an equal volume of air-saturated (21% O_2) buffer [50 mM Hepes (pH 7.4) and 50 mM NaCl]. For β1(1−385) P118A, a small amount of sodium dithionite (2 equiv) was present during mixing, which was found to be necessary to keep the protein fully reduced during subsequent manipulations. The observed O_2 binding rate and the rate of oxidation of β1(1−385) P118A/I145Y were measured using electronic absorption spectroscopy at 37 °C. Spectra were recorded after addition of 150 μL of O_2-saturated buffer to the Fe^{II}-bound protein in 150 μL of anaerobic buffer. The change in the absorbance maximum versus time was plotted, and the data were fit to a single-exponential equation. Dissociation of NO from the heme of sGC was assessed at 25 °C using the CO/dithionite trapping method described previously.[16] The change in the absorbance maximum versus time was plotted, and the data were fit to a double-exponential equation. The time courses shown are representative results of experiments repeated two to six times for each construct.

Resonance Raman Spectroscopy. RR spectra were recorded for samples in spinning NMR tubes via backscattering geometry at room temperature. The protein (∼10 μM heme) was in 50 mM Hepes (pH 7.4), 50 mM NaCl, 1 mM DTT, and 150 μM YC-1, where indicated. The excitation wavelengths at 430 nm (for ligand-free samples) and 413 nm (for CO-bound samples) were obtained by frequency doubling, using a nonlinear lithium triborate crystal, of a Ti:sapphire laser (Photonics Industries International TU-UV), which was pumped by the second harmonic of a Q-switched Nd:YLF laser (Photonics Industries International, GM-30−527). For CO-bound samples, the laser power at the sample was kept to a minimum (<1 mW) by using a cylindrical lens to avoid the photolysis of bound CO. For

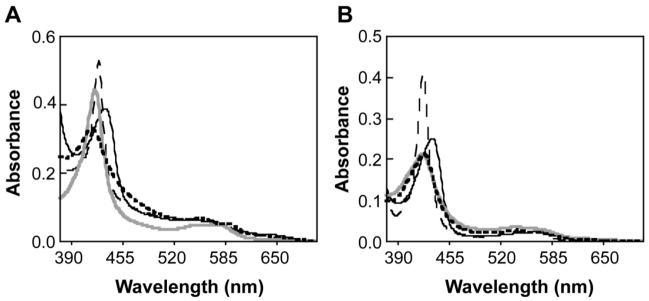

Figure 2. Spectroscopic characterization of sGC chimeras. Electronic absorption spectra of α1/*Tt*_β1 (A) and α1/Gcy-33_β1 (B) at 20 °C. Data for Fe^{II}-unligated (black solid line), Fe^{II}—CO (black dashed line), Fe^{II}—NO (gray solid line), and Fe^{II}—O_2 (black dotted line) complexes are shown.

ligand-free samples, the laser power at the sample was 2−3 mW. Scattered light was collected and focused onto a single spectrograph (SPEX 1269) equipped with a CCD detector (Roper Scientific) operating at −110 °C. Spectra were calibrated with dimethylformamide and DMSO-d_6. Grams A/I (Thermo-Galactic) was used to analyze the spectra.

RESULTS AND DISCUSSION

sGC is a heterodimeric hemoprotein in which each protein subunit consists of four distinct domains (Figure 1A). Proteins with homology to each of the four domains have been elucidated by X-ray crystallography, but there is no structure of the full-length, multidomain protein. In this work, sGC chimeras were designed and characterized to evaluate the structural and functional similarity between sGC and prokaryotic and eukaryotic homologues of sGC and to illuminate aspects of interdomain communication in lieu of a full-length sGC structure.

Characterization of sGC Chimeras. Previous studies have shown that the β1 PAS, CC, and catalytic domains are essential to protein dimerization, while the N-terminal H-NOX domain is essential to gaseous ligand sensing (reviewed in ref 17). When NO binds to the rat sGC H-NOX domain, the level of cGMP synthesis increases several hundred-fold. To determine if guanylate cyclase activity can be regulated by β1 H-NOX domain homologues, the β1 H-NOX domain in rat sGC was replaced with bacterial and worm H-NOX domains. Specifically, three different H-NOX proteins were fused to the β1 PAS-CC-C domain (Figure 1B): *Tt*Tar4H H-NOX, *V. cholerae* VCA0720 H-NOX, and *C. elegans* Gcy-33 H-NOX (*Tt*_β1, *Vc*_β1, and Gcy-33_β1, respectively). The β1 sequence was replaced with *Tt* H-NOX, *Vc* H-NOX, and Gcy-33 H-NOX sequences with 17, 25, and 27% identity, respectively (determined with Lasergene, DNAStar, Inc.). The *Tt* H-NOX domain has the advantage of being an O_2-binding H-NOX domain whose structure has been determined, while the *V. cholerae* domain is a non-O_2-binding prokaryotic H-NOX domain with greater sequence homology to the β1 H-NOX domain, although no structure has yet been determined. The heme domain from Gcy-33 has not been biochemically characterized, but it is known to be an atypical guanylate cyclase (reviewed in ref 18) that mediates an O_2-dependent behavior in worms.[19] This observation, in addition to the presence of a tyrosine at position 145 (rat β1 numbering), strongly suggests the protein binds O_2.[20]

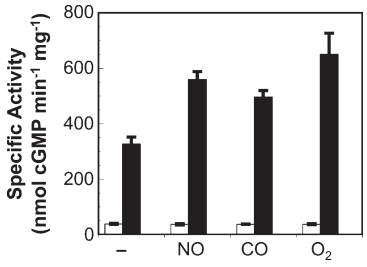

Figure 3. Activity of sGC chimeras. Activity of α1/*Tt*_β1 (white) and α1/Gcy-33_β1 (black) in the presence and absence of NO, CO, and O_2 at 25 °C. Samples of Fe^{II}-unligated protein contained 100 μM sodium dithionite.

The fusion proteins were cloned and then coexpressed with the rat α1 subunit in a Sf9/baculovirus system. The resulting chimeric heterodimer was purified using Ni-NTA metal affinity chromatography, where the tag is on the α1 protein, followed by anion-exchange chromatography. All constructs purified as heterodimers and were greater than 95% pure based on SDS−PAGE. Both prokaryotic chimeras were expressed and purified with yields that were 2−3-fold greater than that of rat α1β1, suggesting that domain swapping might be a useful method for increasing protein yields. The α1/*Tt*_β1 heterodimer as isolated had an electronic absorption maximum between 418 and 420 nm (Table 1). This species is likely the Fe^{II}—O_2 complex on the basis of its similarity to other O_2-bound heme proteins.[21,22] After reduction with sodium dithionite, the ferrous-unligated protein was found to form six-coordinate complexes with O_2, CO, and NO (Figure 2 and Table 1). The ability to bind O_2 and the formation of a six-coordinate Fe^{II}—NO complex demonstrates that the α1/*Tt*_β1 chimera has properties more like those of the bacterial *Tt* H-NOX protein[22] than those of the mammalian β1 H-NOX protein.[6] The α1/*Vc*_β1 heterodimer was isolated as a mixture of apoprotein and heme-bound protein. After reconstitution with heme, the protein formed a six-coordinate complex with CO and a five-coordinate complex with NO, similar to the wild-type *Vc* and β1 H-NOX domains.[6,22] α1/Gcy-33_β1 was isolated heme-bound and required reduction with sodium dithionite to form a reduced Fe^{II}-unligated species. After reduction, the Soret maximum shifted in the presence of NO, CO, and O_2 to 422, 421, and 418 nm, respectively (Figure 2). Biochemical characterization of full-length Gcy-33 has not been reported, so these results cannot be compared to those for the wild-type protein; however, the deviations of these Soret values from those of wild-type α1β1 suggest that the *C. elegans* atypical cyclase forms six-coordinate complexes with NO, CO, and O_2. This indicates that Gcy-33 has biochemical properties similar to those of the related *Drosophila* atypical guanylate cyclase, Gyc-88E,[23] and supports in vivo data that suggest the protein functions as an O_2 sensor in worms.[19]

To determine if the mammalian H-NOX domain homologues can regulate guanylate cyclase activity, we assessed cGMP synthesis in the presence of various heme ligands. The α1 and β1 catalytic domains formed a functional dimer because each chimera exhibited a basal activity (Table 2). Interestingly, α1/Gcy-33_β1 exhibited a basal activity (326 nmol min^{-1} mg^{-1}) that was significantly greater than the α1β1 basal activity (50−100 nmol min^{-1} mg^{-1}). The atypical cyclase Gyc-88E homodimer also exhibited a relatively high basal activity when compared to that of α1β1.[23] While all of the chimeras exhibited a

Table 2. Activity of sGC Chimeras in Various Ligation States at 25 °C

protein	Fe^{II} complex	specific activity (nmol of cGMP min^{-1} mg^{-1})	*x*-fold change (Fe^{II}-X/Fe^{II}-unligated)	*x*-fold change (with YC-1/without YC-1)
α1/β1	Fe^{II}-unligated[b]	58 ± 21	1	5
	Fe^{II}−NO	6054 ± 2303	77	19
	Fe^{II}−CO	124 ± 20	2	31
α1/*Tt*_β1	Fe^{II}-unligated	38 ± 2	1	1
	Fe^{II}−NO	36 ± 3	1	1
	Fe^{II}−CO	37 ± 0.3	1	1
	Fe^{II} + O_2	37 ± 2	1	1
α1/*Vc*_β1[a]	Fe^{II}-unligated	44 ± 1	1	1
	Fe^{II}−NO	55 ± 14	1	1
α1/Gcy-33_β1	Fe^{II}-unligated	326 ± 25	1	ND[c]
	Fe^{II}−NO	560 ± 28	1.7	ND[c]
	Fe^{II}−CO	495 ± 24	1.5	ND[c]
	Fe^{II} + O_2	650 ± 76	2	ND[c]

[a] α1/*Vc*_β1 reconstituted with heme. [b] Fe^{II}-unligated data in the presence of 100 μM sodium dithionite. [c] Not determined.

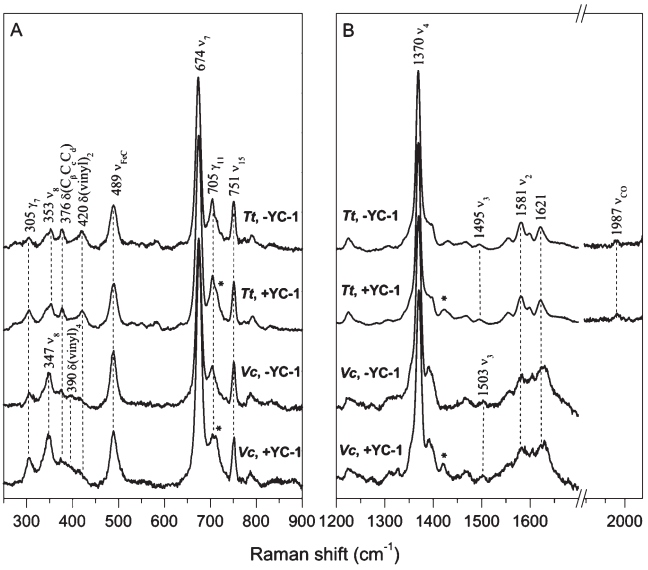

Figure 4. Resonance Raman spectra of the α1/*Tt*_β1 and α1/*Vc*_β1 chimeric heterodimers in the Fe^{II}−CO state. Low-frequency (A) and high-frequency (B) regions are shown for constructs in the absence and presence of YC-1 as indicated. The asterisk denotes bands from DMSO. The ν_{Fe-CO} and ν_{CO} stretching modes are indicated in the low- and high-frequency regions, respectively.

basal activity, NO did not activate α1/*Tt*_β1 or α1/*Vc*_β1. Additionally, α1/*Tt*_β1 was not activated by CO or O_2, and YC-1 did not activate the protein in the unligated, Fe^{II}−CO, or Fe^{II}−NO states (Table 2). YC-1 is a small molecule that synergistically activates sGC in the presence of CO and NO.[24] Thus, replacement of the β1 H-NOX domain with either the *T. tengcongensis* or *V. cholerae* bacterial H-NOX domain abolished the sensitivity of these chimeric sGCs to NO. However, cGMP synthesis of α1/Gcy-33_β1 increased 1.5−2-fold in the presence of NO, CO, and O_2 (Figure 3). Therefore, this atypical guanylate cyclase H-NOX domain maintains some β1-like function when fused to the β1 PAS, CC, and catalytic domains.

The absence of enzyme sensitivity to NO, CO, and O_2 in the rat−bacteria chimeras suggests that ligand binding to these proteins does not induce the same conformational change that is observed with the α1β1 heterodimer. Several factors could contribute to this loss of sensitivity: the communication between the heme binding pocket and the catalytic domains may be disrupted, the prokaryotic H-NOX domains could utilize a different allosteric mechanism of domain regulation, or the prokaryotic H-NOX domains could undergo a conformational change upon NO binding that is distinct from that of the β1 H-NOX domain. To further address these possibilities, resonance Raman (RR) spectroscopy was used to evaluate how the mammalian sGC PAS, CC, and catalytic domains influence the H-NOX heme environment in the context of the chimeric proteins.

Table 3. Resonance Raman Frequencies and Mode Assignments for Various Heme Proteins in the Fe^{II}−CO Ligation State[a]

protein	ν_2	ν_3	ν_4	ν_{Fe-CO}	ν_{CO}	ref
α1β1	1582	1496	1371	473/493	1968/1988	25
Tt H-NOX	1580	1494	1369	490	1989	22
α1/*Tt*_β1	1581	1495	1370	489	1987	*c*
Vc H-NOX	1578	1492	1367	491	1985	22
α1/*Vc*_β1	1582	1503	1370	489	ND[b]	*c*

[a] Vibratins in inverse centimeters. [b] Not determined. [c] From this work.

RR spectroscopy has been previously used to examine the heme environment of *Tt* H-NOX, *Vc* H-NOX, and rat α1β1.[22,25] The RR spectra of α1/*Tt*_β1 and α1/*Vc*_β1 were recorded for this work and compared to the previously published spectra. RR spectra of the Gcy-33 construct could not be obtained because of the high background fluorescence of the sample. The Fe^{II}−CO spectrum of α1/*Tt*_β1 shows that the ν_{FeC} and ν_{CO} frequencies are observed as single bands at 489 and 1987 cm^{-1}, respectively (Figure 4 and Table 3). These values are similar to those reported for the *Tt* H-NOX Fe^{II}−CO complex (490 and 1989 cm^{-1}, respectively).[22] Additionally, the heme skeletal markers in the high-frequency region and the porphyrin conformation-sensitive bands in the low-frequency region are similar to those observed with wild-type *Tt* H-NOX. The RR spectrum did not change upon addition of YC-1, indicating that the small molecule does

dx.doi.org/10.1021/bi200341b |*Biochemistry* 2011, 50, 4281–4290

not bind to this protein or YC-1 is no longer able to induce a conformational change within the heme pocket when it binds. This result is in agreement with the activity studies (vide infra), which showed that YC-1 did not activate the protein.

The Fe^{II}−CO RR spectrum of α1/*Vc*_β1 shows that the ν_{FeC} frequency is observed at 489 cm^{-1} (Figure 4), which is similar to the value reported for wild-type *Vc* H-NOX (491 cm^{-1}).[22] The weak ν_{CO} mode was not observed because of the high fluorescence background of the sample; however, on the basis of the ν_{FeC} frequencies of both α1/*Tt*_β1 and α1/*Vc*_β1, it seems that the anomalously low level of backbonding in α1β1[25] cannot be induced in the prokaryotic H-NOX domains with fusion to the β1 subunit. Interestingly, some heme skeletal marker bands in the high-frequency region shifted from the *Vc* H-NOX values such that they are closer to the values for α1β1 (Table 3). Specifically, ν_2, ν_3, and ν_4 upshift by 4, 11, and 3 cm^{-1}, respectively, and this shows that the *Vc* H-NOX heme environment is indeed influenced by the presence of the PAS, CC, and catalytic domains. Addition of YC-1 produces no spectral change, except for a broadening of the ν_{FeC} band, possibly signaling a minor species with an altered Fe−CO conformation.

YC-1 is thought to bind to the N-terminus of the α1 subunit,[26−28] and this binding event is known to affect the sGC heme conformation.[29,30] Some communication between this binding site and the heme pocket also occurs in the α1/*Vc*_β1 chimera, but this communication is not sufficient to induce activity changes as evidenced by the lack of YC-1-induced activation (Table 2). Together, these RR results suggest that the non-O_2-binding prokaryotic H-NOX domain shares a more homologous structure with the rat β1 H-NOX domain than the O_2-binding prokaryotic H-NOX domain. This would allow the *Vc* H-NOX domain to respond to the β1 PAS, CC, and catalytic domains and undergo a modest conformational change upon YC-1 binding.

The observation that the *Tt* H-NOX domain was apparently unaffected by fusion to the β1 protein shows that some H-NOX proteins do not have the ability to retain even partial function with domain swapping. Perhaps the mechanism of regulation between O_2-binding and non-O_2-binding prokaryotic H-NOXs is too divergent to allow for the retention of function. Conversely, when fused to the β1 protein, the predicted O_2-binding eukaryotic H-NOX domain from a guanylate cyclase was responsive to the presence of NO, O_2, and CO. This argues for some commonality in the mechanism of activation in O_2-binding and non-O_2-binding guanylate cyclases, but the varying degree of ligand-induced activation in α1β1 and α1/Gcy-33_β1 highlights the mechanistic and/or structural differences between these two classes of sGCs.

Critical Heme Pocket Residues. To further probe the influence of the sGC PAS, CC, and catalytic domains on the H-NOX ligand binding properties and heme environment, we conducted site-directed mutagenesis experiments on mammalian sGC domain truncations, β1(1−194) and β1(1−385), and the full-length protein. The β1(1−194) construct contains the H-NOX domain alone, and the β1(1−385) construct contains the H-NOX, PAS, and CC domains (Figure 1A). Two residues in the sGC heme pocket were chosen for site-directed mutagenesis experiments aimed at probing the involvement of the PAS, CC, and catalytic domains in heme ligand binding. Investigations with the O_2-binding H-NOX domain from *T. tengcongensis* have revealed a proximal pocket proline (Pro118 in the rat β1 numbering system) that is important for maintaining the heme conformation[12,13] (Figure 1C). In addition to affecting the protein heme conformation, mutation of proline 118 to alanine in *Tt* H-NOX increases O_2 affinity[12] and increases the proximal Fe−His bond strength.[13] Residue 145 (in the rat β1 numbering system) is another critical residue in H-NOX proteins (Figure 1C). Generally, in O_2-binding H-NOX proteins, position 145 is a tyrosine, while an isoleucine or leucine is most commonly present in non-O_2-binding H-NOX proteins like β1. A kinetic study showed that Tyr145 is critical for O_2 binding in *Tt* H-NOX.[31] To probe the function of this distal pocket residue in β1, we replaced Ile145 with a tyrosine in β1(1−385) (I145Y). This mutation produced a protein that was capable of binding O_2;[31] however, further studies showed that the same mutation in the full-length α1β1 heterodimer did not produce an O_2-binding protein.[32,33] In this work, a comparative study with different sGC β1 chain lengths (Figure 1A) was conducted with modification of conserved heme pocket residues 118 and 145.

Table 4. Electronic Absorption Peak Positions for Various sGC β1 Mutants in α1β1 and H-NOX Domains at 25 °C[a]

protein	sample	Fe^{II}	Fe^{II}−NO	Fe^{II}−CO	Fe^{II}−O_2	ref
α1β1	wild-type	431	399	423	–	36
	β1 P118A	428	399	420	–	*b*
	β1 I145Y	429	**416**/399	423	–	32
β1(1−385)	wild-type	431	399	423	–	7
	β1 P118A	424	398	420	–	*b*
	β1 I145Y	428	**400**/417	422	417	31, *b*
	β1 P118A/ β1 I145Y	425	399	420	417	*b*
β1(1−194)	wild-type	431	398	423	–	6
	β1 P118A	428	398	421	–	*b*
	β1 I145Y	428	400	420	–	*b*

[a] Peak positions in nanometers. [b] This work. The most abundant species of a mixture is shown in bold.

Ligand Binding to β1 P118A and β1 I145Y Mutants in Full-Length α1β1 and H-NOX Domain Constructs. Ligand binding and O_2 reactivity in Pro118 and Ile145 mutants of α1β1, β1(1−385), and β1(1−194) were examined. The electronic absorption maxima for the Fe^{II}, Fe^{II}−NO, and Fe^{II}−CO complexes in α1β1 and H-NOX domain mutants are reported in Table 4. Unlike the *Tt* H-NOX P118A mutant, all β1 P118A mutants were isolated with a substoichiometric amount of heme, determined by the ratio of the Soret maximum (428 nm) to the total protein absorbance (280 nm) compared to that of the wild-type protein. Pro118 would appear to be important for heme affinity in sGC α1β1, but not as critical for that in *Tt* H-NOX. Mutants isolated with a substoichiometric amount of heme were successfully reconstituted. All mutants were then reduced with sodium dithionite, and these reduced proteins exhibited absorbance maxima between 424 and 431 nm (Figure S1 of the Supporting Information). After exposure to CO, the absorbance maxima shifted to 420−423 nm, indicative that all formed a six-coordinate Fe^{II}−CO complex. Both α1β1 P118A and β1(1−194) P118A form a stable five-coordinate complex with NO after displacement of the proximal histidine residue, while β1(1−385) P118A oxidizes rapidly in the presence of either NO or O_2. Characterization of β1 P118A mutants before and after reconstitution confirms that this procedure did not affect the ligand binding properties of the protein.

Table 5. Comparison of Kinetic Parameters for Various sGC β1 Mutants in $\alpha1\beta1$ and H-NOX Domains at 37 °C

protein	sample	observed $k_{on}(O_2)$ (μM^{-1} s^{-1})	k_{ox} (s^{-1})
$\alpha1\beta1$	wild-type	NO[a]	NO[a]
	$\beta1$ P118A	NO[a]	NO[a]
	$\beta1$ I145Y	NO[a]	NO[a]
$\beta1(1-385)$	wild-type	NO[a]	0.00029 ± 0.00002
	$\beta1$ P118A	NO[a]	17.6 ± 0.3[b]
	$\beta1$ I145Y	~0.00004[c]	0.00020[c]
	$\beta1$ P118A/I145Y	0.00012 ± 0.00003	0.00062 ± 0.00025
$\beta1(1-194)$	wild-type	NO[a]	0.00121[d]
	$\beta1$ P118A	NO[a]	0.1950 ± 0.006
	$\beta1$ I145Y	NO[a]	0.0022 ± 0.0005

[a] Not observed. [b] Rate measured and reported at 10 °C. [c] Rates from ref 31. [d] Rates from ref 6.

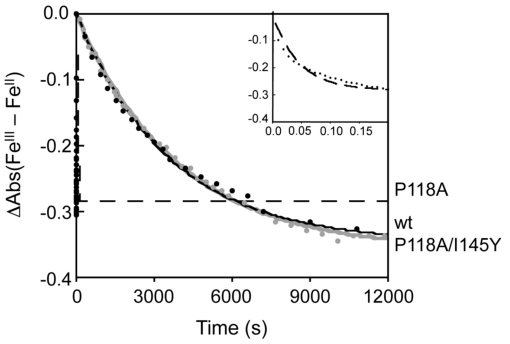

Figure 5. Effect of heme pocket mutation on $\beta1(1-385)$ oxidation rates. Change in absorbance of the Fe^{III} Soret maximum minus the absorbance of the Fe^{II} Soret maximum plotted vs time. Data were fit with a single-exponential equation. Time courses for wild-type (black solid line), P118A (black dashed line), and P118A/I145Y (gray solid line) are shown for $\beta1(1-385)$. The inset shows the data for $\beta1(1-385)$ P118A collected from 0 to 0.2 s.

Enzyme assays were performed to test if alteration of the conserved Pro118 residue affects sGC activity. The mutant had a basal activity that was similar to that of the wild-type protein (Figure S2 of the Supporting Information). This activity increased 40−50-fold in the presence of NO and 1−2-fold upon CO binding. A similar increase was observed with the protein that was not reconstituted with heme, suggesting that the procedure did not affect catalysis. Thus, sGC $\alpha1\beta1$ P118A exhibits a reduction in maximal NO-, CO-, and YC-1-stimulated activity when compared to wild-type sGC. A reduction in maximal enzyme activation was also observed when conserved distal pocket residues were mutated in sGC $\alpha1\beta1$,[16] so not surprisingly, both distal heme pocket and proximal heme pocket (Pro118) residues are important for enzyme activation.

In agreement with a previous report, an $Fe^{II}-O_2$ complex was observed in $\beta1(1-385)$ after the introduction of a tyrosine at position 145;[31] however, the same mutation in either the full-length $\alpha1\beta1$ heterodimer[16,32] or the $\beta1(1-194)$ construct did not produce an O_2-binding protein. Additionally, the I145Y mutation in the three sGC constructs led to different $Fe^{II}-NO$ coordination states. Full-length $\alpha1\beta1$ I145Y is mostly six-coordinate (>85%) at 25 °C,[16,32] and $\beta1(1-385)$ I145Y is mostly five-coordinate (>90%) at 25 °C; however, both are mixtures of five- and six-coordinate complexes. $\beta1(1-194)$ I145Y exclusively formed a five-coordinate complex (Figure S1 of the Supporting Information), suggesting that the tyrosine is positioned differently in this protein compared to the full-length protein. Perhaps the distance from the distal pocket tyrosine to the bound ligand varies such that the protein is unable to form a hydrogen bond in the H-NOX domain. Alternatively, the PAS and CC domains may be involved in preventing the breaking of the Fe−His bond in the full-length protein.

Kinetic Characterization of β1 P118A and β1 I145Y Mutants. In addition to influencing ligand coordination states, distal and proximal heme pocket modifications are known to influence ligand binding kinetics. Heme oxidation in the presence of O_2 and dissociation of NO from the heme were examined in the $\beta1$ mutants. It was previously determined that the $\beta1$ truncation, $\beta1(1-194)$, produces a protein that is more susceptible to oxidation than the full-length protein.[6] In this report, the $\beta1(1-385)$ oxidation rate was 4-fold slower than that of $\beta1(1-194)$ and the full-length protein has no observable oxidation rate under our experimental conditions (Table 5). This demonstrates that the other domains on the $\beta1$ subunit and possibly the $\alpha1$ subunit contribute to the remarkable stability of the Fe^{II} heme state of the $\alpha1\beta1$ heterodimer.

The effect of a mutation within the proximal and distal heme pocket on O_2 binding and oxidation was further examined. Whereas the level of oxidation of $\beta1(1-194)$ and $\beta1(1-385)$ significantly increased (≥100-fold) in the P118A constructs, the $\alpha1\beta1$ P118A heme did not oxidize even after 4 h at 37 °C in the presence of O_2 (Table 5). Additionally, no transient $Fe^{II}-O_2$ complex was observed during the oxidation of either $\beta1(1-194)$ P118A or $\beta1(1-385)$ P118A. The effect of this mutation on the interaction of the $\beta1$ H-NOX truncations with O_2 is more consistent with *Tt* H-NOX than $\alpha1\beta1$. The rate of dissociation of O_2 from *Tt* H-NOX decreased ~6-fold upon mutation of the corresponding proline to alanine.[12] Because the O_2 association rate was unaffected by this mutation, the net effect produced a protein with an increased affinity for O_2. While an observed O_2 off-rate cannot be measured in the $\beta1$ constructs, it is clear that unlike in full-length sGC, mutation of Pro118 in $\beta1(1-194)$ and $\beta1(1-385)$ appreciably altered the affinity of the protein for O_2 and/or lowered the heme reduction potential.

In contrast to the dramatic effect on the H-NOX oxidation rate in the Pro118 mutant, the $\beta1$ I145Y mutation only slightly increased (≤2-fold) the oxidation rate of $\beta1(1-194)$ and did not affect the oxidation rate of $\beta1(1-385)$ (Table 5). In agreement with previous reports, no heme oxidation was observed in the full-length $\alpha1\beta1$ I145Y protein.[16,32] Thus, the Fe^{II} heme center is significantly influenced by the conformation of the full-length heterodimer. Perhaps the $\alpha1$ subunit prevents O_2 from reaching the heme cofactor or influences the iron redox potential.

Because $\beta1(1-385)$ I145Y is known to bind O_2 and mutation of proline 118 was shown to alter O_2 reactivity, the $\beta1(1-385)$ P118A/I145Y double mutant was introduced to determine if the mutations could synergistically alter the affinity for O_2. $\beta1(1-385)$ P118A/I145Y was purified with a substoichiometric amount of heme and was reconstituted as described. The reconstituted protein formed a five-coordinate complex with NO and six-coordinate complexes with both CO and O_2 (Table 4). Interestingly, the oxidation rate and observed O_2

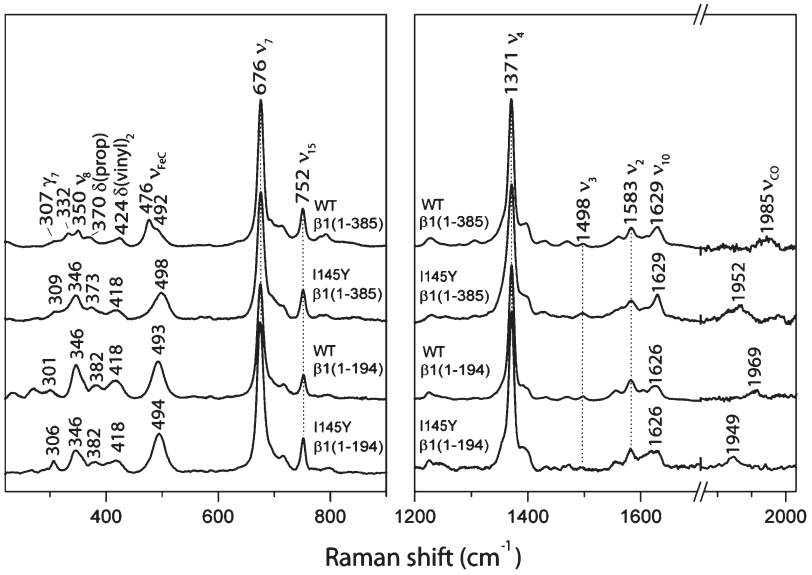

Figure 6. Resonance Raman spectra of wild-type and I145Y $\beta1(1-385)$ and $\beta1(1-194)$ in the $Fe^{II}-CO$ state. Low-frequency (left) and high-frequency (right) regions are shown. The ν_{Fe-CO} and ν_{CO} stretching modes are indicated in the low- and high-frequency regions, respectively.

association rate increased (3- and 5-fold, respectively) in the double mutant when compared to the I145Y mutant (Table 5). The presence of a tyrosine in the heme distal pocket significantly reduced the rate of oxidation of $\beta1(1-385)$ P118A (Figure 5), perhaps by stabilizing O_2 binding at the heme.

To further examine these sGC heme pocket mutants, we measured the observed NO dissociation rate using the CO/dithionite trapping method.[14] Table S1 of the Supporting Information shows that despite significant changes in the susceptibility of the protein to O_2-induced oxidation, the NO dissociation rate in $\beta1(1-194)$ P118A was not very different from the wild-type rate. Dissociation of NO from the $\beta1$ I145Y mutants was also examined (Figure S3 of the Supporting Information). Previous reports have shown that the dissociation rate significantly increased in $\alpha1\beta1$ I145Y;[32] however, there were only slight changes in both the $\beta1(1-194)$ I145Y and the $\beta1(1-385)$ I145Y NO dissociation rates (<2.5-fold). Clearly, the most significant effect of the I145Y mutation was in the NO coordination state and NO dissociation rate of the full-length protein, and this work shows that the heme domain truncations $\beta1(1-194)$ and $\beta1(1-385)$ do not mimic these effects. The varying properties of these mutants in the H-NOX constructs when compared to those of the $\alpha1\beta1$ heterodimer suggest that the full-length protein has additional means to regulate ligand binding and heme reactivity. This regulation may involve a forced structural change in the heme pocket, which could alter potential hydrogen bonding contacts in the mutants.

Probing the $\beta1$ Heme Environment with Resonance Raman Spectroscopy. It is known that mutation of the proximal pocket proline influences the heme conformation and Fe—His bond strength of *Tt* H-NOX.[13] Specifically, several out-of-plane low-frequency modes known to be sensitive to ruffling and saddling deformations exhibited a reduction in intensity and the Fe—His stretching frequency upshifted by 6 cm^{-1}.[13] The resonance Raman spectra of the wild-type and the P118A and I145Y mutants of $\beta1(1-194)$ in the Fe^{II}-unligated state were recorded (Figure S4 of the Supporting Information). Unfortunately, these data could not be compared to the resonance Raman spectra of mutants in full-length sGC because of a high fluorescence background in these samples. In $\beta1(1-194)$ P118A, a slight upshift (2 cm^{-1}) in the ν_{Fe-His} band was observed,[34] whereas here, a slight downshift (3 cm^{-1}) is seen in $\beta1(1-194)$ I145Y when compared to that of the wild-type protein. Therefore, the Fe—His bond strength decreases after mutation of Ile145 and increases after mutation of Pro118 (analogous to the case with *Tt* H-NOX). In agreement with

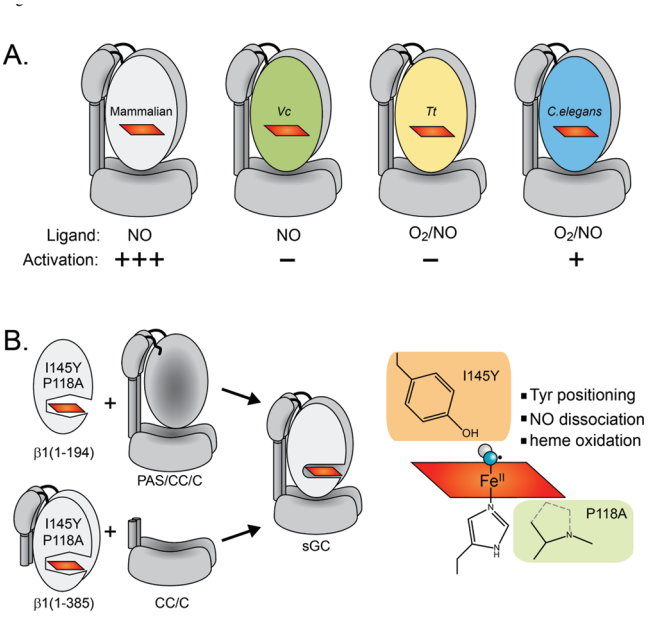

Figure 7. Model of interdomain communication. (A) Fusion of *Vc* or *Tt* H-NOX domains to sGC produces a protein that does not respond to ligand binding at the heme, but fusion of the *C. elegans* Gcy-33 H-NOX domain influences the H-NOX heme environment and enzyme sensitivity to gaseous ligands. (B) Mutation within the heme-binding pocket is influenced by the $\beta1$ PAS, CC, and C domains on the $\alpha1$ and $\beta1$ subunits. These observations indicate that allosteric interactions regulate sGC heme binding properties and enzyme activation.

a previous report, there is no evidence of changes in heme conformation in these mutants based on the relative signal intensities of the low-frequency bands.[34]

The RR $Fe^{II}-CO$ spectra of the $\beta1(1-385)$ and $\beta1(1-194)$ I145Y mutants were also recorded (Figure 6). In $\beta1(1-194)$ I145Y, there is a shift in the ν_{CO} band from 1969 to 1949 cm^{-1}, and in $\beta1(1-385)$ I145Y there is a shift in the wild-type 492 cm^{-1} ν_{FeC} band to 498 cm^{-1}. These shifts are likely due to a positive polar interaction between the introduced tyrosine and the bound CO.[35] This interaction may affect the polarity around the ligand, weaken the contacts of heme propionate with $\beta1$, and/or change the Fe−C−O angle.[34]

The binding of NO and O_2 is significantly influenced by the PAS, CC, and catalytic domains on the basis of electronic absorption spectroscopy and kinetic analysis of site-directed mutants. These domains decrease the heme oxidation rate, perhaps by a mechanism that modulates O_2 accessibility and/or the iron redox potential. Allosteric interactions with these domains induce structural changes in the heme-binding pocket as evidenced by variations in the heme coordination state upon NO binding. Mutational analysis of conserved heme pocket residues also highlights the importance of studying the full-length protein to confirm biochemical predictions based on sGC truncations as some residues, like P118, significantly influence the ligand binding properties of isolated H-NOX proteins but not full-length sGC.

In summary, the $\beta1$ PAS, CC, and catalytic domains can influence the heme environment of *Vc* H-NOX, highlighting the structural similarity between sGC and non-O_2-binding bacterial sGC homologues. Additionally, we determined that Gcy-33 binds oxygen, in addition to NO and CO, and that the $\alpha1$/Gcy-33_$\beta1$ chimera is responsive to varying heme ligation states (Figure 7A). This suggests that atypical guanylate cyclases and NO-sensitive guanylate cyclases have a common mechanism of domain regulation. While the precise molecular mechanism of this regulation remains to be determined, mutational analysis indicates that the allosteric interaction of the $\beta1$ PAS, CC, and catalytic domains on the $\alpha1$ and $\beta1$ subunits affects O_2 reactivity and NO dissociation (Figure 7B), properties that are known to be essential to the physiological function of sGC in mammalian cells.

■ ASSOCIATED CONTENT

Supporting Information. Spectra of sGC mutants (Figure S1), activity of sGC $\alpha1\beta1$ P118A (Figure S2), NO dissociation time courses of $\beta1$ I145Y mutants (Figure S3 and Table S1), and resonance Raman spectra of $\beta1(1-194)$ mutants in the Fe^{II}-unligated state (Figure S4). This material is available free of charge via the Internet at http://pubs.acs.org.

■ AUTHOR INFORMATION

Corresponding Author

*University of California, QB3 Institute, 570 Stanley Hall, Berkeley, CA 94720-3220. Phone: (510) 666-2763. Fax: (510) 666-2765. E-mail: marletta@berkeley.edu.

Present Addresses

#Department of Biological Chemistry and Molecular Pharmacology, Harvard Medical School, Boston, MA 02115.

▽Thermo Fisher Scientific, 355 River Oaks Parkway, San Jose, CA 95134.

Author Contributions

M.B.W. and M.I. contributed equally to this work.

Funding Sources

Funding was provided by National Institutes of Health Grant GM077365 to M.A.M.

■ ACKNOWLEDGMENT

We thank Rosalie Tran and Richard Mathies for preliminary RR characterization of the Fe^{II}-unligated $\beta1(1-194)$ constructs, Bryan Dickinson for preliminary purification of $\beta1(1-194)$ mutants, Eric Underbakke for generating a graphic illustration of our sGC model, and Jonathan Winger for critical input on chimera design.

■ ABBREVIATIONS

sGC, soluble guanylate cyclase; NO, nitric oxide; H-NOX, Heme−Nitric oxide and OXygen binding; PAS, Per/ARNT/Sim; RR, resonance Raman; YC-1, 3-(5′-hydroxymethyl-3′-furyl)-1-benzylindazole; DEA/NO, diethylammonium (*Z*)-1-(*N*,*N*-diethylamino)diazen-1-ium-1,2-diolate; DTT, dithiothreitol; Sf9, *Spodoptera frugiperda*; Hepes, 4-(2-hydroxyethyl)-1-piperazineethanesulfonic acid; DMSO, dimethyl sulfoxide; EIA, enzyme immunoassay; PDB, Protein Data Bank.

■ REFERENCES

(1) Kemp-Harper, B., and Schmidt, H. H. (2009) cGMP in the vasculature. *Handb. Exp. Pharmacol.,* 447–467.

(2) Kleppisch, T., and Feil, R. (2009) cGMP signalling in the mammalian brain: Role in synaptic plasticity and behaviour. *Handb. Exp. Pharmacol.,* 549–579.

(3) Tsai, E. J., and Kass, D. A. (2009) Cyclic GMP signaling in cardiovascular pathophysiology and therapeutics. *Pharmacol. Ther. 122*, 216–238.

(4) Walter, U., and Gambaryan, S. (2009) cGMP and cGMP-dependent protein kinase in platelets and blood cells. *Handb. Exp. Pharmacol.,* 533–548.

(5) Cary, S. P., Winger, J. A., Derbyshire, E. R., and Marletta, M. A. (2006) Nitric oxide signaling: No longer simply on or off. *Trends Biochem. Sci. 31*, 231–239.

(6) Karow, D. S., Pan, D., Davis, J. H., Behrends, S., Mathies, R. A., and Marletta, M. A. (2005) Characterization of functional heme domains from soluble guanylate cyclase. *Biochemistry 44*, 16266–16274.

(7) Zhao, Y., and Marletta, M. A. (1997) Localization of the heme binding region in soluble guanylate cyclase. *Biochemistry 36*, 15959–15964.

(8) Erbil, W. K., Price, M. S., Wemmer, D. E., and Marletta, M. A. (2009) A structural basis for H-NOX signaling in *Shewanella oneidensis* by trapping a histidine kinase inhibitory conformation. *Proc. Natl. Acad. Sci. U.S.A. 106*, 19753–19760.

(9) Ma, X., Sayed, N., Beuve, A., and van den Akker, F. (2007) NO and CO differentially activate soluble guanylyl cyclase via a heme pivot-bend mechanism. *EMBO J. 26*, 578–588.

(10) Nioche, P., Berka, V., Vipond, J., Minton, N., Tsai, A. L., and Raman, C. S. (2004) Femtomolar sensitivity of a NO sensor from *Clostridium botulinum*. *Science 306*, 1550–1553.

(11) Pellicena, P., Karow, D. S., Boon, E. M., Marletta, M. A., and Kuriyan, J. (2004) Crystal structure of an oxygen-binding heme domain related to soluble guanylate cyclases. *Proc. Natl. Acad. Sci. U.S.A. 101*, 12854–12859.

(12) Olea, C., Boon, E. M., Pellicena, P., Kuriyan, J., and Marletta, M. A. (2008) Probing the function of heme distortion in the H-NOX family. *ACS Chem. Biol. 3*, 703–710.

(13) Tran, R., Boon, E. M., Marletta, M. A., and Mathies, R. A. (2009) Resonance Raman spectra of an O_2-binding H-NOX domain reveal heme relaxation upon mutation. *Biochemistry 48*, 8568–8577.

(14) Winger, J. A., Derbyshire, E. R., and Marletta, M. A. (2007) Dissociation of nitric oxide from soluble guanylate cyclase and H-NOX domain constructs. *J. Biol. Chem. 282*, 897–907.

(15) Derbyshire, E. R., and Marletta, M. A. (2007) Butyl isocyanide as a probe of the activation mechanism of soluble guanylate cyclase. Investigating the role of non-heme nitric oxide. *J. Biol. Chem. 282*, 35741–35748.

(16) Derbyshire, E. R., Deng, S., and Marletta, M. A. (2010) Incorporation of tyrosine and glutamine residues into the soluble guanylate cyclase heme distal pocket alters NO and O_2 binding. *J. Biol. Chem. 285*, 17471–17478.

(17) Derbyshire, E. R., and Marletta, M. A. (2009) Biochemistry of soluble guanylate cyclase. *Handb. Exp. Pharmacol.*, 17–31.

(18) Morton, D. B. (2004) Invertebrates yield a plethora of atypical guanylyl cyclases. *Mol. Neurobiol. 29*, 97–116.

(19) Zimmer, M., Gray, J. M., Pokala, N., Chang, A. J., Karow, D. S., Marletta, M. A., Hudson, M. L., Morton, D. B., Chronis, N., and Bargmann, C. I. (2009) Neurons detect increases and decreases in oxygen levels using distinct guanylate cyclases. *Neuron 61*, 865–879.

(20) Boon, E. M., and Marletta, M. A. (2005) Ligand specificity of H-NOX domains: From sGC to bacterial NO sensors. *J. Inorg. Biochem. 99*, 892–902.

(21) Antonini, E., and Brunori, M. (1971) *Hemoglobin and myoglobin in their reactions with ligands*, North-Holland Publishing Co., Amsterdam.

(22) Karow, D. S., Pan, D., Tran, R., Pellicena, P., Presley, A., Mathies, R. A., and Marletta, M. A. (2004) Spectroscopic characterization of the soluble guanylate cyclase-like heme domains from *Vibrio cholerae* and *Thermoanaerobacter tengcongensis*. *Biochemistry 43*, 10203–10211.

(23) Huang, S. H., Rio, D. C., and Marletta, M. A. (2007) Ligand binding and inhibition of an oxygen-sensitive soluble guanylate cyclase, Gyc-88E, from *Drosophila*. *Biochemistry 46*, 15115–15122.

(24) Ko, F. N., Wu, C. C., Kuo, S. C., Lee, F. Y., and Teng, C. M. (1994) YC-1, a novel activator of platelet guanylate cyclase. *Blood 84*, 4226–4233.

(25) Deinum, G., Stone, J. R., Babcock, G. T., and Marletta, M. A. (1996) Binding of nitric oxide and carbon monoxide to soluble guanylate cyclase as observed with resonance Raman spectroscopy. *Biochemistry 35*, 1540–1547.

(26) Derbyshire, E. R., Fernhoff, N. B., Deng, S., and Marletta, M. A. (2009) Nucleotide regulation of soluble guanylate cyclase substrate specificity. *Biochemistry 48*, 7519–7524.

(27) Hu, X., Murata, L. B., Weichsel, A., Brailey, J. L., Roberts, S. A., Nighorn, A., and Montfort, W. R. (2008) Allostery in recombinant soluble guanylyl cyclase from *Manduca sexta*. *J. Biol. Chem. 283*, 20968–20977.

(28) Stasch, J. P., Becker, E. M., Alonso-Alija, C., Apeler, H., Dembowsky, K., Feurer, A., Gerzer, R., Minuth, T., Perzborn, E., Pleiss, U., Schroder, H., Schroeder, W., Stahl, E., Steinke, W., Straub, A., and Schramm, M. (2001) NO-independent regulatory site on soluble guanylate cyclase. *Nature 410*, 212–215.

(29) Li, Z. Q., Pal, B., Takenaka, S., Tsuyama, S., and Kitagawa, T. (2005) Resonance Raman evidence for the presence of two heme pocket conformations with varied activities in CO-bound bovine soluble guanylate cyclase and their conversion. *Biochemistry 44*, 939–946.

(30) Martin, E., Czarnecki, K., Jayaraman, V., Murad, F., and Kincaid, J. (2005) Resonance Raman and infrared spectroscopic studies of high-output forms of human soluble guanylyl cyclase. *J. Am. Chem. Soc. 127*, 4625–4631.

(31) Boon, E. M., Huang, S. H., and Marletta, M. A. (2005) A molecular basis for NO selectivity in soluble guanylate cyclase. *Nat. Chem. Biol. 1*, 53–59.

(32) Martin, E., Berka, V., Bogatenkova, E., Murad, F., and Tsai, A. L. (2006) Ligand selectivity of soluble guanylyl cyclase: Effect of the hydrogen-bonding tyrosine in the distal heme pocket on binding of oxygen, nitric oxide, and carbon monoxide. *J. Biol. Chem. 281*, 27836–27845.

(33) Rothkegel, C., Schmidt, P. M., Stoll, F., Schroder, H., Schmidt, H. H. H. W., and Stasch, J. P. (2006) Identification of residues crucially involved in soluble guanylate cyclase activation. *FEBS Lett. 580*, 4205–4213.

(34) Ibrahim, M., Derbyshire, E. R., Marletta, M. A., and Spiro, T. G. (2010) Probing soluble guanylate cyclase activation by CO and YC-1 using resonance Raman spectroscopy. *Biochemistry 49*, 3815–3823.

(35) Spiro, T. G., Ibrahim, M., and Wasbotten, I. H. (2008) CO, NO and O_2 as vibrational probes of heme protein active sites. In *The smallest biomolecules: Diatomics and their interactions with heme proteins* (Ghosh, A., Ed.) pp 96−123, Elsevier, Amesterdam.

(36) Denninger, J. W., and Marletta, M. A. (1999) Guanylate cyclase and the NO/cGMP signaling pathway. *Biochim. Biophys. Acta 1411*, 334–350.